Contents lists available at ScienceDirect

Journal of Luminescence

journal homepage: www.elsevier.com/locate/jlumin

Ratiometric luminescence thermometry with different combinations of emissions from Eu^{3+} doped $Gd_2Ti_2O_7$ nanoparticles

Vesna Lojpur, Sanja Ćulubrk, Miroslav D. Dramićanin*

University of Belgrade, Vinča Institute of Nuclear Sciences, P.O. Box 522, 11001 Belgrade, Serbia

ARTICLE INFO

Article history:
Received 28 October 2014
Received in revised form
22 December 2014
Accepted 9 January 2015

Keywords:
Thermometry
Luminescence
Pyrochlores
Rare earths
Nanoparticles

ABSTRACT

Herein, Eu^{3+} doped $Gd_2Ti_2O_7$ nanoparticles were tested for application in ratiometric luminescence thermometry. It is shown that two combinations of emissions: one that uses two emissions of Eu^{3+} ions and one that uses one emission of Eu^{3+} ions and trap emission of $Gd_2Ti_2O_7$ provide thermometry over the 303–423 K temperature range with relative sensitivities between 0.14% K^{-1} and 0.95% K^{-1}. Thermometry based on two Eu^{3+} emissions from $^5D_0$ to $^5D_1$ levels has a higher relative sensitivity, but lower absolute sensitivity than thermometry based on one Eu^{3+} emission and trap emission of $Gd_2Ti_2O_7$. The tested material is prepared by Pechini-type polymerized complex route and is composed of agglomerated nanoparticles of ~30–50 nm in size with pure-phase cubic structure (space group Fd-3m) as evidenced from electron microscopy and X-ray diffraction measurements.

1. Introduction

Luminescence thermometry is most commonly performed through relative emission intensity measurements (ratiometric intensity measurements; fluorescence intensity ratio—FIR) [1–5]. This type of measurements is insensitive to fluctuations of excitation light or other changes in measurement conditions, and more importantly, it is self-referencing (i.e., these types of measurements do not have to refer to any temperature standard) [5]. Ideally, one of the used emissions should be independent of temperature (internal reference) and, then, a calibration between the ratios of emissions is indicative of temperature.

When used with rare earth ion-doped materials, this technique involves the use of emissions that originate from two closely spaced, "thermally coupled" excited energy levels of the rare earth ions. The relative population of these levels follows a Boltzmann-type distribution and it is dependent on the temperature and the energy difference between levels (energy gap) [2,6]. The main mechanism behind "thermally coupled" energy levels is thermalization: when two energy levels of the RE activator are closely separated by a difference of ~2000 cm^{-1} or less, the upper level will not fluoresce at low temperatures since electrons do not have enough energy to bridge the energy gap. As the temperature increases, the upper level becomes populated and hence the emission from this level gradually increases in intensity at the expense of the lower level population.

Recently, the new concept of ratiometric luminescence thermometry that exploits trap emission of the host as a self-referencing standard and the emission of the activator ions as temperature indicator has been demonstrated using TiO_2 nanopowders doped with Eu^{3+} ions [7] and Sm^{3+} ions [8], and Zn_2SiO_4 doped with Mn^{2+} ions [9]. This concept provided high relative sensitivities and the possibility to perform luminescence thermometry with activator ions which have only single intense emission band (as in the case of Mn^{2+}:Zn_2SiO_4 [9]).

Here, we aimed to compare performance of two above mentioned concepts of ratiometric luminescence thermometry with Eu^{3+} doped $Gd_2Ti_2O_7$ nanoparticles. $Gd_2Ti_2O_7$ exhibit notable luminescence after incorporation of rare earth ions [10–16]. In this cubic-type host rare-earth dopants replace Gd^{3+} ions in crystallographic sites with a strict center of symmetry (D_{3d}) [16]. The emission spectrum of Eu^{3+} doped $Gd_2Ti_2O_7$ consists of emissions from Eu^{3+} spin-forbidden f–f electronic transitions [15] and trap emission of $Gd_2Ti_2O_7$ induced by the presence of oxygen vacancies [17]. Therefore, both ratiometric intensity concepts are feasible with this material.

2. Experimental

2.1. Material synthesis procedure

$Gd_2Ti_2O_7$:5 at% Eu^{3+} nanopowder was prepared by Pechini-type polymerized complex route, described in detail in our previous work [15]. In brief, this synthesis method is based on polyesterification between citric acid (CA) and ethylene glycol. For

---

* Corresponding author.
E-mail address: dramican@vinca.rs (M.D. Dramićanin).

http://dx.doi.org/10.1016/j.jlumin.2015.01.027

Please cite this article as: V. Lojpur, et al., J. Lumin. (2015), http://dx.doi.org/10.1016/j.jlumin.2015.01.027

synthesis of $Gd_2Ti_2O_7$:5 at% Eu^{3+} nanopowder, titanium (IV)-isopropoxide, gadolinium(III)-nitrate, citric acid and ethylene glycol were mixed in 1:1:5:20 M ratio. First, titanium (IV)-isopropoxide (Alfa Aesar, 97%) was dissolved in ethylene glycol (Lach-Ner, 99%) under constant magnetic stirring. Then citric acid (Kemika, 99.5%) was added to the solutions and stirred until complete dissolution was achieved. After that, appropriate amounts of Gd_2O_3 (Alfa Aesar, 99.9%) and Eu_2O_3 (Alfa Aesar, 99.9%) were dissolved in hot, concentrated nitric acid, evaporated to dryness and joined with titanium (IV)-isopropoxide/EG/CA mixture. Mixtures were stirred for 1 h at 60 °C until they became transparent and further heated at 130 °C for a few hours to promote polymerization. Black, amorphous resins were fired at 350 °C for 30 min. At the end, pure phase of $Gd_2Ti_2O_7$:5 at% Eu^{3+} nanopowder was obtained after annealing at 880 °C for 4 h and naturally furnace cooling to the room temperature.

2.2. Instruments and measurements

Phase composition of the sample was checked with X-ray powder diffraction measurement performed on a Rigaku Smartlab diffractometer. Diffraction data were collected in the 2θ range from 10° to 90°, counting 0.7°/min in 0.02 steps. The morphological features and chemical purity were investigated by means of scanning electron microscopy (SEM JEOL, JSM-6610LV) with INCA energy dispersive X-ray analysis. For this purpose the powder sample was dispersed on Cu holder and sputtered with Au. Transmission electron microscopy (TEM) is conducted using JOEL-JEM 2100 instrument equipped with LaB_6 cathode and operated with 200 kV. For TEM measurements powders were used without any additional preparation. Photoluminescence spectra were collected using a Fluorolog-3 Model FL3-221 spectrofluorometer system (Horiba Jobin-Yvon), over the temperature range from 293 to 433 K. The photoluminescence measurements were performed under continuous excitation from a 450 W Xenon lamp at a wavelength of 393 nm. The samples were placed in a custom-made temperature controlled furnace, and emission spectra were collected via an optical fiber bundle. The temperature of the samples was controlled within the accuracy of ± 0.5 °C by a temperature control system utilizing proportional-integral-derivative feedback loop equipped with T-type thermocouple for temperature monitoring. Experimental setup shown in Fig. 1, consists of the following parts: 1. Lamp, 2. Detector, 3. Monochromator, 4. Optical fiber, 5. Lens, 6. Sample, 7. Oven, 8. T-regulator, 9. Controller and 10. PC.

3. Results and discussion

Pyrochlores with formula $A_2B_2O_7$ crystallize into a face-centered cubic lattice with space group Fd-3m, No 227. Unit cell contains eight molecules ($Z=8$) and four crystallographically nonequivalent sites. The A cation (usually of ionic radius ~1 Å) is eight-coordinated and located within scalenohedra (distorted cubes) that contain six equally spaced O atoms at a slightly shorter distance from the central cation. The smaller B cation (ionic radius ~0.6 Å) is six-coordinated and located within a trigonal antiprism with all six anions at equal distances from the central cation. In the pyrochlore structure, D_{3d} symmetry of the metal cation point group requires that these two polyhedra are neither octahedra nor cubes (but trigonal antiprisms and scalenohedra), even though many authors do refer to them as octahedral and cubic coordination polyhedra [15]. XRD patterns of $Gd_2Ti_2O_7$:5 at% Eu^{3+} powder are presented in the Fig. 2. The main diffraction peaks are indexed according to the ICCD card No. 01-074-9640. There were no peaks related to any other phases indicating sample without impurities. High intensity is a consequence of high crystallinity of the powder.

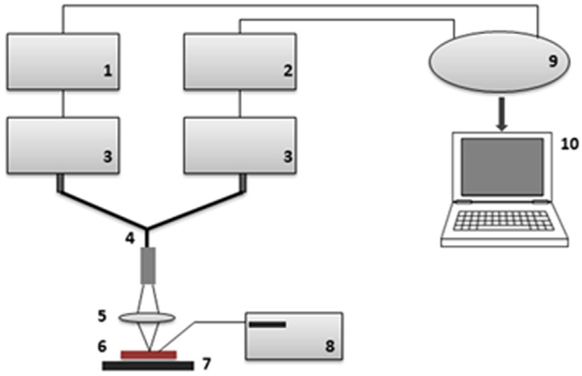

Fig. 1. Experimental setup for temperature dependent photoluminescence measurement.

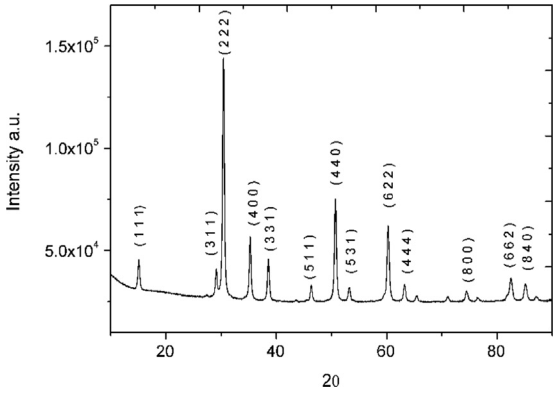

Fig. 2. XRD diffraction patterns for $Gd_2Ti_2O_7$:5 at% Eu^{3+} powder indexed according to the ICCD card No. 01-074-9640.

Morphology of the sample obtained through Pechini-type polymerized complex route was showed in Fig. 3. The micrograph provided by SEM analysis, Fig. 3a, indicated that $Gd_2Ti_2O_7$:5 at% Eu^{3+} consists of large chunks with a size of several tens of microns. The elements distribution determined by the energy dispersive X-ray mapping analysis, examined chemical homogeneity of the powder as shown in Fig. 3b. The elemental maps of Gd, TiO and Eu confirmed uniform distribution of all elements throughout the material. The EDX spectrum showed in Fig. 3c revealed the presence of Eu^{3+} ions and the purity of rare earth doped $Gd_2Ti_2O_7$.

Further magnification was followed by TEM measurements. The TEM micrograph is presented in Fig. 3d and revealed that chunks are entirely composed of nanoparticles. It is evident that particles are agglomerated and have irregular, round and rectangular shapes. Size of nanoparticles is mostly around 30–50 nm.

Luminescence spectra of $Gd_2Ti_2O_7$:5 at% Eu^{3+} powders measured as a function of temperature (293–423 K) are shown in the Fig. 4. Two distinct spectral regions can be observed: high energy broad band spectral region (400–550 nm) that belongs to the trap emission of the $Gd_2Ti_2O_7$ host and the low energy spectral region that belongs to emission of Eu^{3+} ions. Emission of dopant is composed of distinctive bands peaking at 589 nm, 597 nm ($^5D_0 \rightarrow {}^7F_1$) 611 nm and 627 nm ($^5D_0 \rightarrow {}^7F_2$) that arise from spin-forbidden electron transition. In addition, small intensity emission from $^5D_1 \rightarrow {}^7F_1$ transition can be observed at about 535 nm. It is clearly seen from the Fig. 4that dopant emission is extremely sensitive to temperature, showing a rapidly decreasing intensity with the temperature increase while changes of trap emission are minimal with the change of temperature in the measured range. Small changes in trap emission intensities are a consequence of slight changes in optical properties of the host with temperature such as band gap energy, reflectivity and changes of

Please cite this article as: V. Lojpur, et al., J. Lumin. (2015), http://dx.doi.org/10.1016/j.jlumin.2015.01.027